Electronic and magnetic structure of $LaMnO_3$ from hybrid periodic density-functional theory

D. Muñoz,[1,2] N. M. Harrison,[1] and F. Illas[2]
[1]*Department of Chemistry, Imperial College of Science, Technology and Medicine, London SW7 2AZ, United Kingdom*
[2]*Departament de Química Física i Centre de Recerca en Química Teòrica, Universitat de Barcelona i Parc Científic de Barcelona, C/ Martí i Franquès 1, E-08028 Barcelona, Spain*

(Received 26 March 2003; revised manuscript received 21 July 2003; published 27 February 2004)

The electronic and magnetic structures of the $LaMnO_3$ compound have been studied by means of periodic calculations within the framework of spin polarized hybrid density-functional theory. In order to quantify the role of approximations to electronic exchange and correlation three different hybrid functionals have been used which mix nonlocal Fock and local Dirac-Slater exchange. Periodic Hartree-Fock results are also reported for comparative purposes. The *A*-antiferromagnetic ground state is properly predicted by all methods including Hartree-Fock exchange. In general, the different hybrid methods provide a rather accurate description of the band gap and of the two magnetic coupling constants, strongly suggesting that the corresponding description of the electronic structure is also accurate. An important conclusion emerging from this study is that the nature of the occupied states near the Fermi level is intermediate between the Hartree-Fock and local density approximation descriptions with a comparable participation of both Mn and O states.

DOI: 10.1103/PhysRevB.69.085115 PACS number(s): 71.15.−m, 71.15.Mb, 75.30.Et, 75.47.Gk

I. INTRODUCTION

The $LaMnO_3$ perovskite is the parent compound for a series of manganese based materials with general formula $A_{1-x}B_xMnO_3$. Upon doping with alkaline-earth cations these materials exhibit unusually large variations of the electric and thermal conductivity induced by the presence of external magnetic fields. This phenomenon discovered in 1994 by Jin *et al.*[1] is usually referred to as colossal magnetoresistance. The origin of this technologically important property is essentially unknown and the role of the doping although decisive is also unclear. Nevertheless, the relationship between the large magnetoresistance in these oxides and a unique metal-insulator transition, in which a complex interplay of magnetic, charge, and orbital degrees of freedom is involved, is nowadays well established.[2] Clearly, the understanding of the metal-insulator transitions requires a rather detailed knowledge of the electronic structure of the parent compound material. The pioneering neutron diffraction work of Wollan and Koehler[3] unambiguously revealed that the undoped $LaMnO_3$ is an *A*-type antiferromagnetic (AAF) insulator, with an antiferromagnetic coupling in the *b* direction and a ferromagnetic coupling in the *ac* planes. Upon doping, this magnetic ordering changes leading to a ferromagnetic cell or to several types of antiferromagnetic cells, depending on the amount of doping. Simultaneously, and again depending on the doping, the compound exhibits a mixed valence character. These features, combined with the several possible metal-insulator transitions, result in a rich and extremely complex phase diagram.

Early attempts to explain the electronic structure and magnetic properties of $LaMnO_3$ involved the ideas of the double-exchange (DE) mechanism, proposed by Zener[4] and extensively developed by Anderson and Hasegawa[5] and de Gennes.[6] This mechanism can be easily understood using the language of valence bond theory in which the total *N*-electron wave function is written as a superposition of instantaneous situations (usually referred to as resonating forms) each described by an electronic configuration (a Slater determinant) written in the atomic orbitals basis set (see, for instance, Ref. 7). In this theoretical framework the DE mechanism is nothing but the contribution to the total energy of the ground state of the Hamiltonian matrix elements coupling the Mn^{3+}-O^{2-}-Mn^{4+} and Mn^{4+}-O^{2-}-Mn^{3+} resonating forms; hereafter referred to as Ψ_{right} and Ψ_{left}. These two resonating forms have identical diagonal matrix elements and hence one can think in terms of the quasidegenerate perturbation theory. The coupling term involves the interaction of either Ψ_{left} and Ψ_{right} with the Mn^{3+}-O^{-}-Mn^{3+} resonating form, hereafter referred to as Ψ_{CT} because it involves a charge transfer from the oxygen to the metal. The second-order contribution of Ψ_{CT} to the ground state energy involves the $\langle\Psi_{\text{left}}|\hat{H}|\Psi_{\text{CT}}\rangle\langle\Psi_{\text{CT}}|\hat{H}|\Psi_{\text{right}}\rangle$ product and hence the DE mechanism is often interpreted as a simultaneous excitation from an electron from Mn^{3+} to O^{2-} and from O^{2-} to Mn^{4+}. However, one should keep in mind that the DE mechanism does not really involve a double excitation; it rather implies the product of two single excitations. Expressed in this way the DE mechanism bears some similarities to the superexchange (SE) mechanism. However, in the case of SE some of the second-order contributions involve the square of the matrix element coupling the $Mn^{3+}(\alpha)$-O^{2-}-$Mn^{3+}(\beta)$ and $Mn^{3+}(\beta)$-O^{2-}-$Mn^{3+}(\alpha)$ resonating forms, where α and β denote the spin of the four unpaired electrons per magnetic center. In the DE mechanism the coupling involves a charge transfer excitation whereas the SE mechanism occurs through the ionic Mn^{4+}-O^{2-}-Mn^{2+} resonating form. The difference between the SE and DE mechanisms lies in the strength of the coupling which is much larger in the latter provided the unpaired t_{2g} electrons have parallel spins.

While useful for understanding purposes these models have a number of limitations, especially when attempting to provide a quantitative picture. The SE mechanism only explains the sign of the magnetic coupling constant[8,9] while DE

is just one of the possible physical mechanisms involved in the electron transport process in doped $LaMnO_3$. In fact, studies by Millis *et al.*[10] have shown that DE is not enough to explain the enormous magnetoresistive effect exhibited by the doped manganites. Based on the existence of orbital ordering in this compound, several alternative mechanisms have been proposed.[11] The orbital ordering occurs because of the breaking of the degeneracy of the Mn^{3+} d manifold in the $t_{2g}^3 e_g^1$ ground state electronic configuration. This symmetry breaking is related to the existence of the cooperative Jahn-Teller effect, which distorts the MnO_6 octahedra present in the crystalline structure of the material by the differential elongation of some of the Mn-O bonds. Hence, it is not rigorous to denote the d orbitals as t_{2g} or e_g although this notation will continue to be used for convenience. This particular orbital ordering is responsible for the A-type antiferromagnetic structure present in the undoped material. The doping of the structure introduces Mn^{4+} ions into the lattice, which are not affected by the Jahn-Teller effect, thus changing the orbital ordering in the lattice and resulting in a change in the nature of the ground state and the magnetic ordering.

In order to investigate the origin of the remarkable properties of the manganites, the electronic structure of $LaMnO_3$ has been studied by means of different methods of solid state physics. In particular, band structure calculations have been carried out within the local density approximation (LDA) of density-functional theory (DFT). However, results are catastrophic, since the LDA describes the insulating cubic phase of this compound as a conductor and yields much too small a band gap for the orthorhombic phase.[12] This is not surprising since the LDA fails to predict the proper electronic ground state of many narrow band systems.[13,14] Further refinements to the exchange-correlation functional, like the generalized gradient approximation (GGA), do not fully repair the artifacts introduced by the LDA.[15] This is in line with results reported for ionic systems with localized d open shells such as NiO which is described as a metal at the LDA level and with too small a band gap at the GGA level, still indicating either an erroneous metallic or semiconducting behavior.[16–18] An approach which supplements the LDA with an effective on-site repulsion, often referred to as LDA $+U$, is also widely used.[19,20] This approximation also improves the gap and lattice constant, but its usual implementation involves the introduction of two semiempirical parameters.[20] A different and sophisticated post-LDA method is the *GW* approximation. It focuses on repairing the self-energy correction in a more controlled, formally acceptable way. It successfully introduces a gap in NiO, which in the self-consistent implementation of the theory is ~ 3.7 eV,[21] in excellent agreement with experiment. It is interesting to note that the self-consistency condition is important, as the earlier non-self-consistent implementation of the theory gives a gap of ~ 5.5 eV which is significantly larger than experiment.[22] The *GW* approximation also improves the magnetic moments and density of states relative to the LDA.

The methods described above all start from the LDA and attempt to repair the tendency of the LDA to excessively delocalize the electron density[23] which results in the underestimation of the band gap. A different procedure consists in choosing an alternative starting point. In this respect, the Hartree-Fock (HF) method in its spin polarized (or spin unrestricted) implementation provides a suitable zero order approximation since it properly describes the insulating character of this class of materials,[24–28] including $LaMnO_3$.[29,30] However, in direct contrast to the LDA, the unrestricted Hartree-Fock (UHF) method considerably overestimates the band gap. The fundamental reason for this deficiency in the UHF method is the neglect of electron correlation. For molecular systems electronic correlation effects can be systematically included by means of the configuration interaction expansion of the N-electron wave function. Unfortunately, for extended systems, this approach cannot be used in general although substantial progress has been made in the last few years.[31–33] At first sight a logical way to improve the UHF description is to use exact Fock exchange in conjunction with a correlation functional as suggested by various authors.[34,35] Unfortunately, this approach does not significantly improve the description of the band gap.[18] Very significant progress has been made through the introduction of hybrid exchange density functionals in which the exact Fock exchange is mixed with a given exchange functional and the correlation is also treated within the density functional framework. These functionals appear to be very well suited to describe not only the band gap[18,36,37] but also the magnetic coupling constants[37,38,39] of these insulating ionic systems.

From the previous discussion it is clear that hybrid DFT calculations provide an excellent basis for the development of a new understanding of the complex electronic structure of materials such as $LaMnO_3$. In this paper periodic calculations based on UHF and several hybrid DFT approximations for various magnetic phases of orthorhombic $LaMnO_3$ are presented. In particular the band gap, the physical nature of the highest occupied bands, and the magnetic coupling constants obtained by the different theoretical approaches are discussed and compared to available experimental data.

II. COMPUTATIONAL DETAILS

The electronic structure of $LaMnO_3$ is studied by periodic UHF and various DFT methods using a massive parallel version of the CRYSTAL package.[40] This computational code makes use of local basis sets of Gaussian-type orbitals (GTOs) as used in standard quantum chemistry calculations. All electrons of Mn and O atoms are explicitly included in the calculations whereas a nonrelativistic pseudopotential is used to describe the inner electrons of the La atom. For Mn and O we use the GTO basis sets used previously by Dovesi *et al.*[41] in their study of the $CaMnO_3$ compound. The basis set for Mn contains $20s$, $12p$, and $5d$ primitive GTOs, contracted to $1s$, $4sp$, and $2d$ through a 8/6411/41 contraction scheme; for O a $14s$, $6p$ primitive set is contracted to $1s$ and $3sp$ shells using a 8/411 contraction. In the case of La, the pseudopotential designed by Dolg *et al.*,[42] and adapted to the CRYSTAL code, is used in order to ease the computational effort. The basis set associated to this pseudopotential starts from $5s$, $4p$, and $3d$ primitives contracted to $3s$, $2p$, and $1d$ through a 311/31/3 scheme. The cutoff threshold param-

eters of CRYSTAL for Coulomb and exchange integral evaluations (ITOL1 to ITOL5) have been set to 7, 7, 7, 7, and 14, respectively. The integration in reciprocal space has been carried out on a Pack-Monkhurst grid of shrinking factor 8, yielding a mesh of 36 *k* points in the irreducible Brillouin zone. The numerical thresholds used to ensure the numerical convergence of the self-consistent-field procedure were set to 10^{-6} a.u. for the one-electron eigenvalues and 10^{-7} a.u. for the total energy. In the DFT methods an even-tempered set of auxiliary Gaussian basis functions has been used to fit the density in order to compute the electron-electron Coulomb and exchange-correlation contributions to the total energy. For manganese, the auxiliary basis set contains 14 *s*-type basis functions with exponents between 0.1 and 7000.0, seven *p*-type functions with exponents between 0.5 and 20.0, five *d*-type functions with exponents between 0.25 and 6.0, three *f*-type functions with exponents between 0.35 and 4.3, and finally three *g*-type functions with exponents between 0.45 and 3.3. In the same way, the auxiliary basis for oxygen contains 14 *s*-type functions with exponents between 0.07 and 4000.0, and one *p*, one *d*, and one *f* function, each with an exponent 0.5. Finally, the auxiliary basis set for the La pseudoatom consists of 14 *s*-type functions with exponents between 0.1 and 6000.0, five *p*-type functions with exponents between 0.5 and 30.0, three *d*-type functions with exponents between 0.5 and 3.0, one *f*-type function with exponent 0.5, and one *g*-type function with exponent 0.3.

The only input datum used in all calculations is the crystalline structure of $LaMnO_3$, which has been studied by several groups.[43–45] In the present study, the recent neutron diffraction parameters determined by Rodriguez-Carvajal *et al.* have been used throughout. It is important to notice that upon changing the temperature the structure of this compound undergoes several phase transformations. At low temperatures $LaMnO_3$ exhibits an orthorhombic symmetry defined by the *Pnma* crystallographic group. In this structure the MnO_6 octahedral building units are distorted as a result of the Jahn-Teller effect and appear slightly tilted relative to each other. Upon heating above 790 K, the structure becomes ''cubic'' and the space group changes to *Pbnm*. For the purposes of the present investigation, the *Pnma* experimental structure has always been considered. In order to compare results obtained using different methods calculations have been performed at the experimentally determined structure. The UHF optimized cell parameter and fractionary coordinates of cell atoms are in fairly close agreement with experiment and so this is expected to have a negligible effect on the description of the band gap or of the physical nature of the bonding and character of the highest occupied bands. Nevertheless it is important to realize that magnetic properties are more strongly affected by the choice of the crystal structure. In fact, the dependence of the magnetic coupling constant *J* on the distance between nearest neighbor magnetic centers is usually $J \sim r^{-n}$ with $12 \geqslant n \geqslant 6$, depending on the compound.[46] Therefore, it is preferable to use the experimental structure and thus avoid any bias introduced by the use of a different crystal structure. We will return to this point in the forthcoming discussion.

Three different computational DFT methods have been used, which are the commonly used B3LYP approach[47] and the Fock-35 and Fock-50 approaches as defined by Moreira *et al.*[37] The B3LYP energy functional has the form

$$E_{xc}^{\mathrm{B3LYP}} = (1-A)E_x^{\mathrm{Slater}} + AE_x^{\mathrm{HF}} + BE_x^{\mathrm{Becke}} + CE_{\mathrm{corr}}^{\mathrm{LYP}} + (1-C)E_{\mathrm{corr}}^{\mathrm{VWN}}, \quad (1)$$

where E_x^{Slater} is the Dirac-Slater local exchange, E_x^{HF} the Hartree-Fock exchange, E_x^{Becke} the gradient part of the Becke gradient corrected exchange functional,[48] $E_{\mathrm{corr}}^{\mathrm{LYP}}$ the correlation functional of Lee, Yang, and Parr,[49] and $E_{\mathrm{corr}}^{\mathrm{VWN}}$ the local density approximation to the electron gas correlation functional following the parametrization of Vosko, Wilk, and Nusair.[50] In the B3LYP method the *A, B, C* parameters of the exchange-functional are fitted to reproduce experimental thermochemical data with $A \sim 20\%$. It is worth pointing out that quite surprisingly, the B3LYP hybrid functional is able to reproduce the thermochemistry of molecules containing transition metal elements although no transition metal compounds were included in the data set used in the fit.[51–54] In a similar way, the Fock-35 and Fock-50 approaches combine a 35% or a 50% of Fock exchange with the Slater exchange and also use the standard Vosko-Wilk-Nusair correlation functional. For a more complete discussion about these hybrid approaches the reader is referred to Moreira *et al.*[37]

III. ELECTRONIC STRUCTURE

In order to study the electronic structure of $LaMnO_3$ one needs first to determine the electronic ground state. In highly localized systems in which the electronic, orbital, structural and spin degrees of freedom are strongly coupled there are typically a large number of possible stable states of the self consistent procedure. In order to determine the ground state spin polarized calculations have been carried out starting from several different electronic configurations and the corresponding electron density iterated to self consistency, the different spin polarized solutions obtained are described in more detail in Sec. IV. The electronic ground state is predicted to be the AAF phase which involves antiferromagnetic coupling between Mn-O layers in the *a-b* plane and ferromagnetic coupling within a given *a-c* layer. This prediction is in agreement with experiment[3] and independent of the method of calculation chosen (UHF or the several hybrid functionals explored in the present work). However, the calculated band gap (Δ) of $LaMnO_3$ has been found to be extremely sensitive to the treatment of exchange and correlation; this is clearly seen in the plots of the total density of states reported in Fig. 1. The UHF method predicts $\Delta = 13.0$ eV, which is much larger than the observed value of $\Delta = 1.7$ eV.[55,56]

One can understand the overestimate of the band gap in UHF theory and its underestimate in LDA/GGA approximations to DFT from a number of points of view. Here we note that the two approaches are radically different in their treatment of electronic self-interaction. In the LDA/GGA approach the occupied states are pushed up in energy by self interaction as each state contributes to the total potential; the

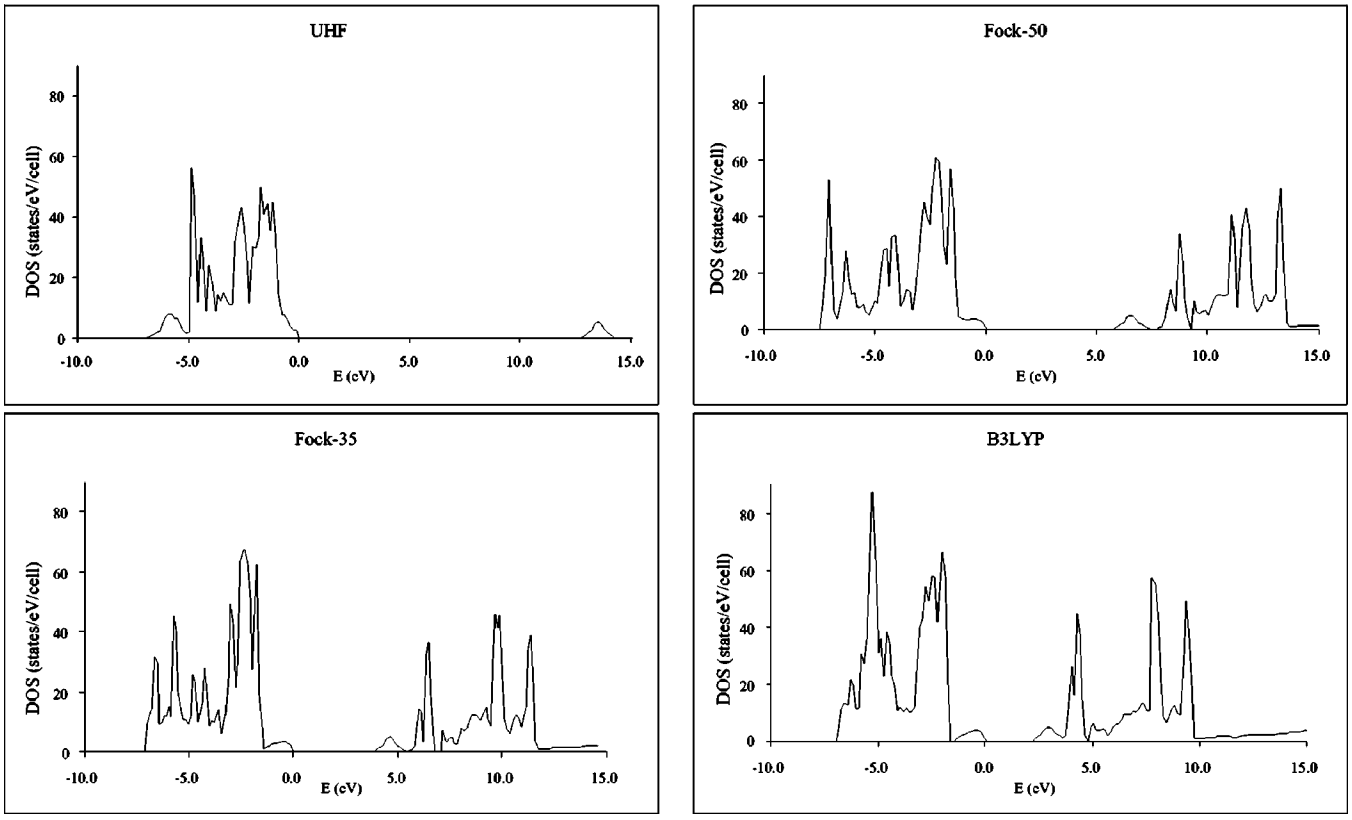

FIG. 1. The total density of states (DOS) for $LaMnO_3$ in the AAF electronic ground state as predicted by the UHF (a), Fock-50 (b), Fock-35 (c), and B3LYP (d) approximations.

unoccupied states are unaffected by this and thus it is quite natural that the band gap is underestimated and that this error is largest in localized systems where the diagonal Coulomb interactions are large. The self-interaction corrected (SIC)-LDA approach introduces explicit nonunitary interactions in an attempt to correct for this error. In the UHF approximation the self-interaction correction appears as the exact cancellation of the diagonal Coulomb and exchange interactions. Here the SIC is overestimated, and the resultant band gap too large, as in reality the on-site Coulomb interaction is screened (or equivalently is modified by electron correlation). Empirically one finds that LDA/GGA band gaps are invariably much smaller than those predicted by the UHF method and in the limit of the LDA implementation of DFT $LaMnO_3$ band gap is predicted to be $\sim$0.2 eV, one order of magnitude smaller than the experimental value.[12,57] Within the SIC point of view the hybrid exchange functionals can be considered to be a crude form of a screened exchange approximation in which the bare diagonal exchange interaction of UHF theory is screened with the semilocally approximated exchange of the LDA and GGA. Certainly the introduction of Fock exchange in the exchange functional has a very large effect as has already been pointed out by several authors.[18,36,37] In fact, the magnitude of the band gap predicted by the different DFT methods varies with the amount of Fock exchange although not in a linear way. From results in Table I one can see that introduction of 50% Fock exchange decreases the UHF value from 13.0 to 5.8, whereas a further reduction to 35% leads to 4.0 eV. Interestingly enough, B3LYP predicts a band gap of 2.3 eV, extremely close to the experimental value even if final state effects are neglected in the calculation of the band gap directly from the band structure. All hybrid exchange functionals predict values of Δ which are reasonably close to experiment. The UHF and LDA approximations represent extremes of an overestimation and an underestimation of the band gap, respectively. It is reasonable to expect that a better description of the magnitude of the band gap implies an overall better description of the electronic structure. Therefore it is important to examine the effect of the amount of Fock exchange mixed into the functional on the qualitative description of the electronic structure and in particular of the density of states (DOS) near the Fermi energy which has been subject of some controversy. In fact, from photoemission spectra Saitoh *et al.*[56] conclude that there are two main and nearly equal

TABLE I. The band gap (Δ), net charge on Mn and O (q_{Mn} and q_{o} in a.u.), and total magnetic moment on Mn (μ_{Mn}) in the AAF electronic ground state. The charges and magnetic moments are obtained from a Mulliken population analysis.

Method	Δ (eV)	q_{Mn} (a.u.)	q_{o} (a.u.)	μ_{Mn} (a.u.)
UHF	13.0	2.18	−1.58	3.96
Fock50	5.8	1.92	−1.46	3.89
Fock35	4.0	1.83	−1.42	3.84
B3LYP	2.3	1.77	−1.38	3.80
Experiment	1.7[56]	—	—	3.87

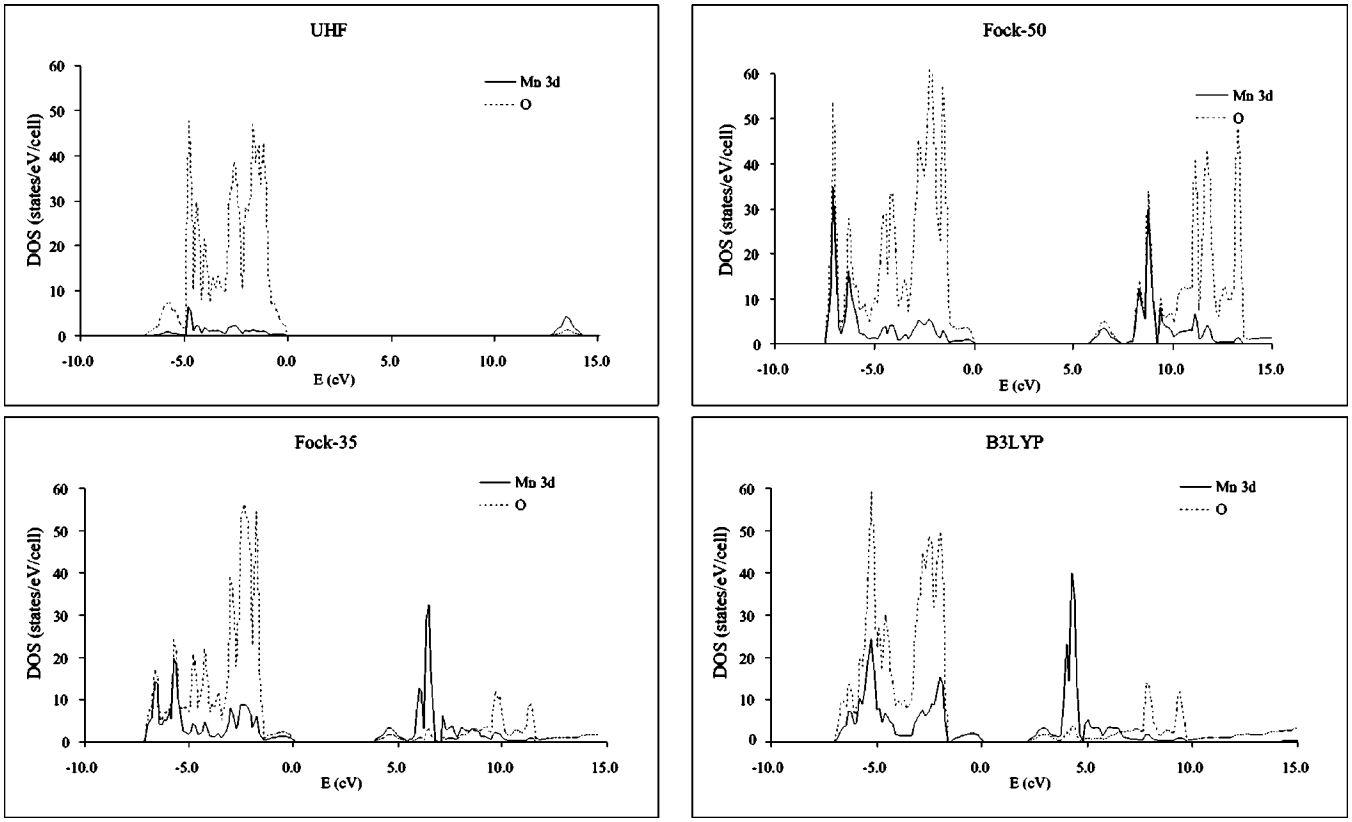

FIG. 2. The local density of states for $LaMnO_3$ in the AAF electronic ground state as predicted by the UHF (a), Fock-50 (b), Fock-35 (c), and B3LYP (d) approximations. The Mn($3d$) and O($2p$) contributions are marked by solid and dashed lines, respectively.

contributions to the DOS near the Fermi energy, these are given formally by the ionic d^4 and formally charge transfer $d^5\underline{L}$ configurations. This picture implies a large covalent contribution to the Mn-O chemical bond and contrasts with the interpretation of Sarma *et al.*,[57] who, based on LDA calculations, suggest a much more metallic description within the *d* band.

To analyze in more detail the structure of the DOS corresponding to the AAF electronic ground state as described by the different methods the total DOS as well as the Mn($3d$) and O($2p$) contributions to the DOS (i.e., the local density of states) are given separately in Figs. 1 and 2. The local density of states (LDOS) obtained by the UHF method [Fig. 2(a)] exhibits a very large contribution of oxygen states near the Fermi energy while the contribution of the Mn *d* orbitals is very small. At the opposite extreme, the LDA calculations of Pickett *et al.*[12] and Sarma *et al.*[57] suggest that the DOS near the Fermi energy is dominated by the Mn *d* orbitals. The different description of the LDOS by UHF and LDA methods is a consequence of a qualitatively different description of the chemical bond. The electronic structure picture arising from the hybrid methods is somewhat intermediate between the HF and LDA methods (Fig. 3), as has been reported for a number of other systems.[18,36,37] The variation in the magnitude of the band gap is accompanied by noticeable changes in the states near the Fermi energy, the *d* bands being shifted towards higher energies by an amount which depends on the extent of Fock exchange included in the method. In this way, the B3LYP method leads to the largest contribution of manganese to the highest occupied energy levels, while the hybrid scheme, having a 50% of the Fock exchange (hereafter referred to as Fock-50), exhibits a DOS which is intermediate between B3LYP and UHF approaches. However, the important point is that the qualitative picture of the electronic structure and of the DOS near the Fermi level predicted by the different hybrid methods is not sensitive to the proportion of Fock exchange used and qualitatively different from either the UHF or the LDA extremes. The fact that the hybrid methodology provides a consistent picture, independent of the precise details of the mixing, and also provides a reasonable estimate of the band gap, is a strong indication that the description is reliable and that both Mn($3d$) and O($2p$) participate in a quite similar proportion to the DOS near the Fermi energy. This conclusion is consistent with a picture of the chemical bond in which both ionic (in the formal valence sense) and covalent (metal-ligand orbital mixing) contributions (or resonating forms) have to be considered and is also consistent with Saitoh *et al.*s interpretation of the photoemission spectra.[56] This picture of the chemical bond in $LaMnO_3$ is also in agreement with the results arising from the Mulliken population analysis carried out for the different total densities (Table I). The absolute value of the net charge is not a quantitative measure of the ionicity as Mulliken charges are strongly dependent on the basis set.[58] However, the variation of the Mulliken charge with the amount of Fock exchange is a reliable measure of changes in the bonding and it indicates a significant reduction of ionicity when going from the UHF method to B3LYP. Interestingly the variation

in the net charge is not paralleled by the variation in the magnetic moment which is relatively insensitive to the mixing and very close to the experimental value.[59] This is in the line of previous investigations on $LaMnO_3$ (Ref. 29) and several other ionic magnetic compounds.[37–39]

IV. MAGNETIC ORDERING AND PHASES

In order to study the magnetic order the widely used broken symmetry approach is adopted. This consists of finding different spin-polarized solutions and, from the corresponding energy differences, deducing the magnitude of the magnetic coupling constants.[25,60] Usually, the different broken symmetry solutions are found by doubling the unit cell in the appropriate direction.[25,26,37,61] However, in the case of $LaMnO_3$ there are several possible broken symmetry solutions within the primitive unit cell. Following the work of Su *et al.*[29] we have chosen to study the four lowest broken symmetry solutions; this will permit a detailed comparison with the previous UHF calculations and allows us to isolate the important effects of the different hybrid functionals on their relative energies. The four broken symmetry solutions correspond to the FM, AAF, CAF, and GAF magnetic cells which are described as follows: FM is associated with the fully ferromagnetic material; AAF corresponds to a ferromagnetic coupling along the *ac* plane with an antiferromagnetic coupling along the *b* axis, CAF corresponds to an antiferromagnetic order in the *ac* plane with a ferromagnetic coupling in the *b* axis, and GAF corresponds to the situation where all spins are antiferromagnetically coupled to their nearest neighbors. In all cases the magnetic orbitals and magnetic order are identical to that discussed in the previous works of Su *et al.*[29] and Nicastro and Patterson[30] Therefore, we will not discuss this point further and will concentrate instead on the effects of the exchange-correlation effect on the energy difference corresponding to the each magnetic phase and to the resulting values of the magnetic coupling constants.

In order to extract the relevant magnetic coupling constants of $LaMnO_3$ from the energy of the different magnetic solutions an Ising model Hamiltonian is considered, which considers the nearest neighbor (J_1) and next-nearest neighbor (J_2) manganese centers,

$$H = -J_1 \sum_{\langle ij \rangle} S_{zi} S_{zj} - J_2 \sum_{\langle kl \rangle} S_{zk} S_{zl}, \tag{2}$$

where S_{zi} stands for the z component of total spin on the magnetic center i and $\langle ij \rangle$ and $\langle kl \rangle$ indicate sums over first and second neighbors, respectively. Notice that with this definition positive (negative) values of the magnetic coupling constant mean ferromagnetic (antiferromagnetic) interactions. Using the mapping procedure described in previous works[26,60,61] an overdetermined set of three equations and two unknowns is obtained. These are

$$\begin{aligned} E(\mathrm{FM}) - E(\mathrm{AAF}) &= -32J_2, \\ E(\mathrm{GAF}) - E(\mathrm{FM}) &= 64J_1 + 32J_2, \\ E(\mathrm{CAF}) - E(\mathrm{FM}) &= 64J_1. \end{aligned} \tag{3}$$

TABLE II. The energy of the different broken symmetry solutions of $LaMnO_3$ relative to the FM solution for various exchange-correlation approximations. The values are in meV per unit cell containing four Mn centers.

Method	AAF	GAF	CAF
UHF	−5.18	51.21	55.88
B3LYP	−32.16	113.96	121.51
Fock50	−12.16	89.22	93.64
Fock35	−18.85	109.83	115.35

The energy of each magnetic phase has been calculated using spin-polarized Hartree-Fock theory and the three hybrid density functional theory approaches described in Sec. II (Table II). For all of the approaches employed in this work, the lowest energy always corresponds to the AAF phase, in good agreement with the observed ground state. In increasing order of energy one finds the FM, GAF, and CAF phases. The same order of stability is predicted by all four approximations. The UHF results are very close to those reported earlier by Su *et al.*[29] and Nicastro and Patterson,[30] the small deviations probably being due to the use of a different pseudopotential for the La atoms and the slightly different geometry adopted in the current study. Here it is worth emphasizing that the present values for the magnetic coupling constants are all obtained using the experimental geometry. This strategy is different from that used by Nicastro and Patterson, who used the UHF optimized structure. The reason for such a different choice in the current study is the desire to isolate purely geometric effects from those due to varying treatments of exchange and correlation. The strong dependence of the magnitude of the magnetic coupling constants with the geometry was commented upon in Sec. II. Nicastro and Patterson obtained reasonable values for the magnetic coupling constants using the UHF optimized geometry to carry out a rather limited configuration interaction calculation which lacks many of the dynamical correlation effects that have previously been demonstrated to be essential for a reliable and quantitative description of the magnetic coupling constant of a large variety of compounds.[8] Also, it is worth pointing out that although the UHF optimized geometry is noticeably close to the experimental one, small variations in the structural parameters have a much larger

TABLE III. The magnetic coupling constants $\mathbf{J}_1$ and $\mathbf{J}_2$, in meV, for various exchange-correlation approximations and using the energy values of all four magnetic phases reported in Table II. Error bars correspond to the standard deviation for the series of values computed from the overdetermined set of equations (3).

Method	$\mathbf{J}_1$	$\mathbf{J}_2$
UHF	0.88±0.01	−0.15±0.01
B3LYP	2.09±0.27	−0.62±0.54
Fock50	1.52±0.09	−0.26±0.17
Fock35	1.91±0.15	−0.38±0.29
Expt. (Ref. 59)	0.83	−0.58

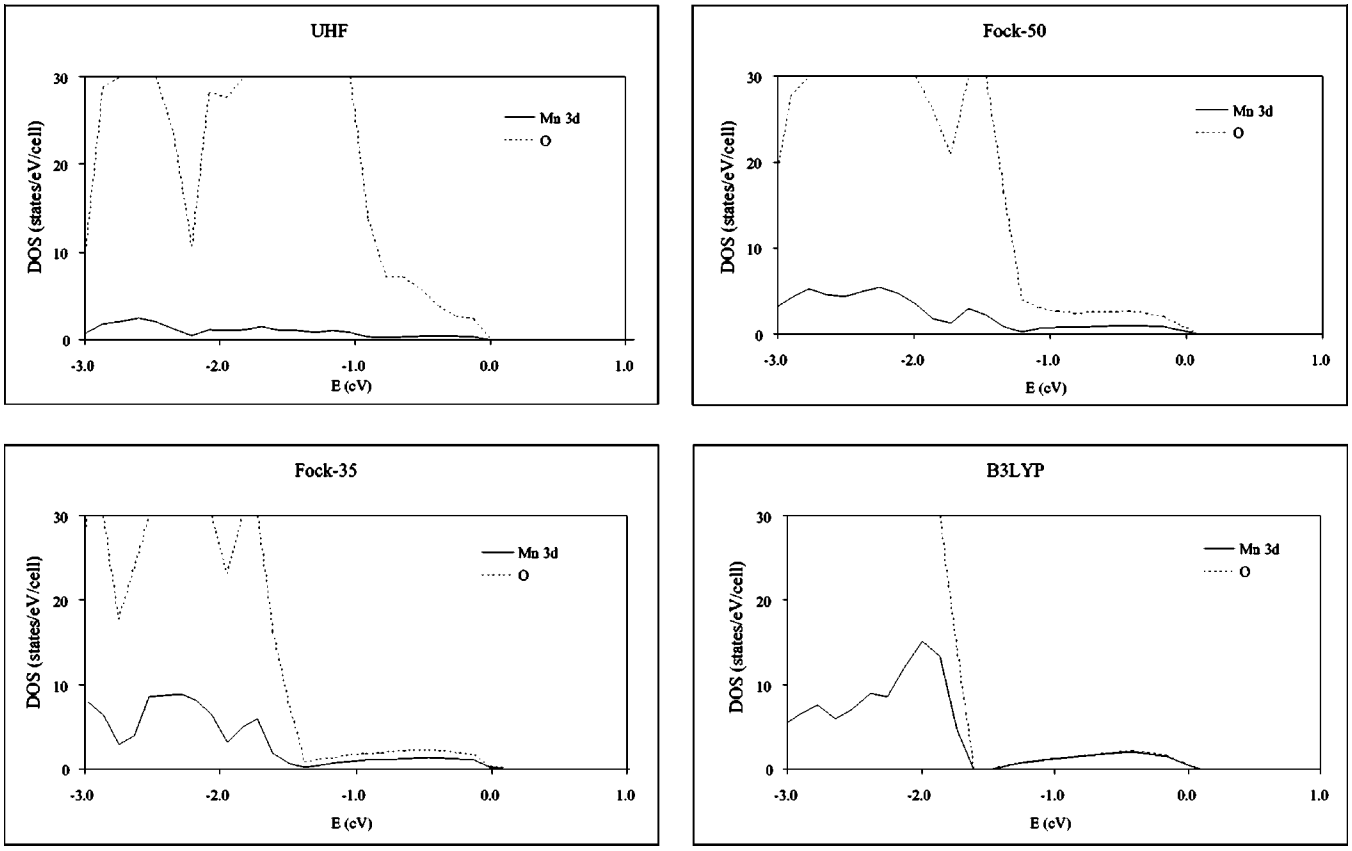

FIG. 3. Detail of the local density of states for $LaMnO_3$ in the AAF electronic ground state near the Fermi level as predicted by the UHF (a), Fock-50 (b), Fock-35 (c), and B3LYP (d) approximations. The Mn($3d$) and O($2p$) contributions are marked by solid and dashed lines, respectively.

effect on the magnitude of the magnetic coupling constants because of the $J \sim r^{-n}$ relationship described above.

The values of J_1 and J_2 are found to be largely dependent on the hybrid functional in agreement with previous findings. Nevertheless, all methods predict the correct sign of each magnetic coupling constant (Table III). From a more quantitative point of view it is found that the three hybrid approaches predict values of J_1 reasonably close to experiment and with little standard deviation [computed from the different J_1 values obtained using any two of the three equations given in Eq. (3)]. The value of J_2 computed from the different hybrid functionals is also in agreement with the experimental value, especially for the B3LYP method, although its standard deviation is slightly larger than the J_1 values (see Table III).

V. CONCLUSIONS

The electronic and magnetic structures of $LaMnO_3$ have been investigated by means of periodic HF and hybrid DFT methods. The value of the band gap, the nature of the highest occupied levels, and the magnitude of the magnetic coupling constants are found to vary strongly with the amount of Fock exchange included in the exchange-correlation method in agreement with previous findings for other strongly correlated systems. Overall, the B3LYP and Fock-35 methods provide a reliable description of the band gap and of the two magnetic coupling constants. This is in line with previous findings showing the decisive role of the exchange functional in the description of the electronic and magnetic structure of these strongly correlated systems.[38,39] The fact that B3LYP and Fock-35 methods are able to quantitatively reproduce the available experimental data strongly suggests that the corresponding description of the electronic structure is also well reproduced. An important implication of this conclusion is that the nature of the occupied states near the Fermi level is intermediate between the UHF and LDA descriptions which favor the participation of Mn or O states, respectively. In the hybrid description the participation of both Mn and O states appears in a similar proportion. This is an important conclusion that needs to be considered when studying the more technologically important doped related compounds.

ACKNOWLEDGMENTS

The authors are indebted to Dr. Jean Paul Malrieu and Dr. Coen de Graaf for fruitful discussions and to Dr. Iberio de P. R. Moreira for critically reading the manuscript with several important suggestions. This research was supported by the Spanish MCyT Grant No. BQU2002-04029-C02-01 and, in part, by *Generalitat de Catalunya* Grant No. 2001SGR-00043. Computer time was provided by the CESCA and CEPBA supercomputing centers, through grants from the

Fundació Catalana de la Recerca and from the *Universitat de Barcelona*. N.M.H. acknowledges the financial support of the European Community for staying in Barcelona through the Improving Human Potential contract No. HPRI-CT-1999-00071 held by the CESCA-CEPBA. CRYSTAL calculations have been carried out on the SP3 parallel machine of the CEPBA-IBM-Research-Institute, of Barcelona. D.M. is indebted to the *Ministerio de Ciencia y Tecnologia* for a predoctoral grant, and F.I. is also grateful to the DURSI of the *Generalitat de Catalunya* for the additional financial support through the *Distinció per a la promoció de la Recerca Universitària*.

[1] S. Jin, T. H. Tiefel, M. McCormack, R. A. Fastnacht, R. Ramesh, and J. H. Chen, Science **264**, 413 (1994).
[2] A. P. Ramirez, J. Phys.: Condens. Matter **9**, 8171 (1997).
[3] E. O. Wollan and W. C. Koehler, Phys. Rev. **100**, 545 (1955).
[4] C. Zener, Phys. Rev. **82**, 403 (1951).
[5] P. W. Anderson and H. Hasegawa, Phys. Rev. **100**, 675 (1955).
[6] P. G. de Gennes, Phys. Rev. **118**, 141 (1960).
[7] I. de P. R. Moreira, N. Suaud, N. Guilhery, J. P. Malrieu, R. Caballol, J. M. Bofill, and F. Illas, Phys. Rev. B **66**, 134430 (2002).
[8] I. de P. R. Moreira, F. Illas, C. J. Calzado, J. F. Sanz, J. P. Malrieu, N. Ben Amor, and D. Maynau, Phys. Rev. B **59**, R6593 (1999).
[9] D. Muñoz, I. de P. R. Moreira, and F. Illas, Phys. Rev. B **65**, 224521 (2002).
[10] A. J. Millis, P. B. Littlewood, and B. I. Shraiman, Phys. Rev. Lett. **74**, 5144 (1995).
[11] J. B. Goodenough, Annu. Rev. Mater. Sci. **28**, 1 (1998).
[12] W. E. Pickett and D. Singh, Phys. Rev. B **53**, 1146 (1996).
[13] K. Terakura, T. Oguchi, A. R. Williams, and J. Klüber, Phys. Rev. B **30**, 4734 (1984).
[14] Z.-X. Shen, R. S. List, D. S. Dessau, B. O. Wells, O. Jepsen, A. J. Arko, R. Barttlet, C. K. Shih, F. Parmigiani, J. C. Huang, and P. A. P. Lindberg, Phys. Rev. B **44**, 3604 (1991).
[15] H. Sawada, Y. Morikawa, K. Terakura, and N. Hamada, Phys. Rev. B **56**, 12 154 (1997).
[16] T. C. Leung, C. T. Chan, and B. N. Harmon, Phys. Rev. B **44**, 2923 (1991).
[17] Ph. Dufek, P. Blaha, V. Sliwko, and K. Schwarz, Phys. Rev. B **49**, 10 170 (1994).
[18] T. Bredow and A. R. Gerson, Phys. Rev. B **61**, 5194 (2000).
[19] V. I. Anisomov, J. Zaanen, and O. K. Andersen, Phys. Rev. B **44**, 943 (1991).
[20] V. I. Anisimov, I. V. Solovyev, M. A. Korotin, M. T. Czyzyk, and G. A. Sawatzky, Phys. Rev. B **48**, 16 929 (1993).
[21] S. Massidda, A. Continenza, M. Posternal, and A. Baldereschi, Phys. Rev. B **55**, 13 494 (1997).
[22] F. Aryasetiawan and O. Gunnarsson, Phys. Rev. Lett. **74**, 3221 (1995).
[23] H. Chevreau, I. de P. R. Moreira, B. Silvi, and F. Illas, J. Phys. Chem. A **105**, 3570 (2001).
[24] M. D. Towler, N. L. Allan, N. M. Harrison, V. R. Saunders, W. C. Mackrodt, and E. Aprà, Phys. Rev. B **50**, 5041 (1994).
[25] J. M. Ricart, R. Dovesi, C. Roetti, and V. R. Saunders, Phys. Rev. B **52**, 2381 (1995); **55**, 15 942(E) (1997).
[26] P. Reinhardt, I. de P. R. Moreira, C. de Graaf, F. Illas, and R. Dovesi, Chem. Phys. Lett. **319**, 625 (2000).
[27] R. Dovesi, C. Roetti, C. Freyria-Fava, M. Prencipe, and V. R. Saunders, Chem. Phys. **156**, 11 (1991).
[28] M. Catti, R. Dovesi, A. Pavese, and V. R. Saunders, J. Phys.: Condens. Matter **3**, 4151 (1991).
[29] Y.-S. Su, T. A. Kaplan, S. D. Mahanti, and J. F. Harrison, Phys. Rev. B **61**, 1324 (2000).
[30] M. Nicastro and C. H. Patterson, Phys. Rev. B **65**, 205111 (2002).
[31] P. Fulde, Adv. Phys. **51**, 909 (2002).
[32] K. Fink and V. Staemmler, J. Chem. Phys. **103**, 2603 (1995).
[33] A. Shukla, M. Dolg, P. Fulde, and H. Stoll, Phys. Rev. B **60**, 5211 (1999).
[34] R. Colle and O. Salvetti, Theor. Chim. Acta **37**, 329 (1975); **53**, 55 (1979).
[35] R. Colle and O. Salvetti, J. Chem. Phys. **79**, 1404 (1993).
[36] J. Muscat, A. Wander, and N. M. Harrison, Chem. Phys. Lett. **342**, 397 (2001).
[37] I. de P. R. Moreira, F. Illas, and R. L. Martin, Phys. Rev. B **65**, 155102 (2002).
[38] R. L. Martin and F. Illas, Phys. Rev. Lett. **79**, 1539 (1997).
[39] F. Illas and R. L. Martin, J. Chem. Phys. **108**, 2519 (1998).
[40] V. R. Saunders, R. Dovesi, C. Roetti, M. Causà, N. M. Harrison, R. Orlando, and C. M. Zicovich-Wilson, CRYSTAL 98 User's Manual, University of Torino, Torino, 1998.
[41] F. Freyria-Fava, Ph. D'Arco, R. Orlando, and R. Dovesi, J. Phys.: Condens. Matter **9**, 489 (1997).
[42] M. Dolg, H. Stoll, A. Savin, and H. Preuss, Theor. Chim. Acta **75**, 173 (1989).
[43] J. B. A. A. Elemans, B. Van Laar, K. R. Van Der Veer, and B. O. Loopstra, J. Solid State Chem. **3**, 238 (1971).
[44] S. Satpathy, Z. S. Popovic, and F. R. Vukajlovic, Phys. Rev. Lett. **76**, 960 (1996).
[45] J. Rodriguez-Carvajal, M. Hennion, F. Moussa, A. H. Moudden, L. Pinsard, and A. Revcolevschi, Phys. Rev. B **57**, R3189 (1998).
[46] L. J. de Jongh and R. Block, Physica B **79**, 569 (1975).
[47] A. D. Becke, J. Chem. Phys. **98**, 1372 (1993).
[48] A. D. Becke, Phys. Rev. A **38**, 3098 (1988).
[49] C. Lee, W. Yang, and R. G. Parr, Phys. Rev. B **37**, 785 (1988).
[50] S. H. Vosko, L. Wilk, and M. Nusair, Can. J. Phys. **58**, 1200 (1980).
[51] A. Ricca and C. W. Bauschlicher, J. Phys. Chem. **98**, 12899 (1994).
[52] T. V. Russo, R. L. Martin, and P. J. Hay, J. Chem. Phys. **102**, 8023 (1995).
[53] L. Rodriguez-Santiago, M. Sodupe, and V. Branchadell, J. Chem. Phys. **105**, 9966 (1996).
[54] P. E. M. Siegbahn and R. H. Crabtree, J. Am. Chem. Soc. **119**, 3103 (1997).
[55] T. Arima, Y. Tokura, and J. B. Torrance, Phys. Rev. B **48**, 17 006 (1993).
[56] T. Saitoh, A. E. Bocquet, T. Mizokawa, H. Namatame, A. Fuji-

mori, M. Abbate, Y. Takeda, and M. Takano, Phys. Rev. B **51**, 13 942 (1995).
[57] D. D. Sarma, N. Shanthi, S. R. Barman, N. Hamada, H. Sawada, and K. Terakura, Phys. Rev. Lett. **75**, 1126 (1995).
[58] P. S. Bagus, F. Illas, C. Sousa, and G. Pacchioni, in *Electronic Properties of Solids using Cluster Models*, edited by T. A. Kaplan and S. D. Mahanti (Plenum, New York, 1995), p. 93.
[59] F. Moussa, M. Hennion, J. Rodriguez-Carvajal, H. Moudden, L. Pinsard, and A. Revcolevschi, Phys. Rev. B **54**, 15 149 (1996).
[60] I. de P. R. Moreira and F. Illas, Phys. Rev. B **55**, 4129 (1997).
[61] C. de Graaf and F. Illas, Phys. Rev. B **63**, 014404 (2001).